ATLANTIS PRESS

Advances in Biological Sciences Research, volume 3

International Conference on Biological Engineering and Pharmacy (BEP 2016)

Amygdala-Prefrontal Connectivity Analysis of Decoding Human Emotion

Wenjie HE
China National Digital Switching System Engineering and Technological Research Center
Zhengzhou, China
e-mail: mulan92@126.com

Haibing BU
China National Digital Switching System Engineering and Technological Research Center
Zhengzhou, China
e-mail: bhblzh@263.net

Zhonglin LI
Department of Radiology
People's Hospital of Zhengzhou University
Zhengzhou, China
e-mail: zhonglinlixd@163.com

Bin YAN*
China National Digital Switching System Engineering and Technological Research Center
Zhengzhou, China
e-mail: ybspace@hotmail.com

Li TONG
China National Digital Switching System Engineering and Technological Research Center
Zhengzhou, China
e-mail: tttocean@163.com

Linyuan WANG
China National Digital Switching System Engineering and Technological Research Center
Zhengzhou, China
e-mail: wanglinyuanwly@163.com

***Abstract*—Functional neuroimaging studies have found that emotion network in patients with some psychiatric and neurological diseases was abnormal. However, human emotion network is extremely complex and understanding of it still remains unclear. So, it's difficult to regulate and remodel emotion network directly. Here, we first estimated the critical connectivity from whole brain functional connectivity, whose seed regions were the structurally and functionally distinct nuclei of amygdala, the basolateral amygdala (BLA) and centromedial amygdala (CMA). And then the critical connectivity was extracted from whole brain functional connectivity using a machine learning method. The experimental results showed that the connectivity between left amygdala and various regions of the prefrontal gyrus, especially right medial superior frontal gyrus, performed better in the classification. Moreover, real time fMRI neurofeedback training also demonstrated that the critical connectivity provided a great contribution for emotion regulation. These findings may be useful support for the connectivity-based emotion regulation training and possibly applied to supplementary treatment of emotion illness.**

Keywords-emotion illness; fMRI; functional connectivity; basolateral amygdala; centromedial amygdala

I. INTRODUCTION

Emotional illness has become one of the top threats to urban mental health, and has affected seriously human work and life, even induced disharmony of society. The typical emotional illness includes major depressive disorder (MDD), social anxiety disorder (SAD), autism spectrum disorder (ASD) and so on [1-3]. For diagnoses of emotional illness, doctors make out a medical certificate according to the Diagnostic and Statistical Manual of Mental Disorders IV (DSM-IV) [4] after asking for the patient's clinical signs and symptoms. So, it's significant to explore a valid and objective biomarker to distinguish, even treat patients with emotional illness.

In recent years, neuroimaging technologies have a speedy development, of which functional magnetic resonance imaging (fMRI) has attracted special attention [5,6]. With the aid of fMRI, neuroscience studies found human high-level cognitive activities, such as emotion, were performed by the brain functional networks. Some psychiatric and neurological diseases could alter functional connectivity in the brain functional network [7-9]. Real-time fMRI neurofeedback (rt-fMRI NF) is a conspicuous intervention approach. It has been suggested that rt-fMRI NF not only could help participants up- or down-regulate activities of brain areas, but also help shape brain functional network [10-12]. But, the regulating effect of brain functional network as feedback signals may not be significant because of lack of pertinence. The emotion network has been explored since the Papez circuit was described [13]. However, which functional connectivity in the emotion network plays the critical role in control of emotion still remains unclear. So, it's necessary to find out the critical connectivity and regulate it by rt-fMRI NF. It seems a trend of treatment of some psychiatric and neurological diseases.

The amygdale, a critical brain region for generation, expression and experience of negative emotions, contains two major nuclei, the basolateral amygdala (BLA) and centromedial amygdala (CMA) [14, 15]. Although BLA and CMA play important roles in emotional processing, they

have different responsibilities in the neural mechanism [16, 17]. In the present study, our goal was to determine whether a data-driven technique could help to discriminate the critical emotional functional connectivity from whole brain functional connectivity, whose seed regions were BLA and CMA. Specially, temporal connectivity patterns were extracted from positive-negative emotional pictures data and used as classification features. Then, due to the sensitivity to subtle and spatially distributed differences in the brain [18], a linear support vector machine (SVM) algorithm was employed to combine the selected features for the critical connectivity diagnosis. Finally, an emotion regulation NF training was used to verify the validity of classification results. Therefore, we hypothesized that the critical connectivity could be used as a biomarker for emotion recognition and regulation.

II. MATERIALS AND METHODS

A. Positive and Negative Emotional Pictures Experiment

- Participants

Twelve healthy volunteers (aged 22-24 years) were recruited from university. All participants had no history of neurological or psychiatric diseases and twenty-twenty vision, and were right-handed. The research protocol was approved by the ethics committee of People's Hospital of Henan Province and conducted at People's Hospital of Henan Province. All subjects gave written informed consent to participate in the study and received financial compensation.

- Experimental Paradigm

The stimuli consisted of positive and negative pictures that were taken from the International Affective Picture Set (IAPS). 60 images (mean and standard deviation for normative valence 7.67±0.28) were used for two positive runs. In the same way, 60 images (mean and standard deviation for normative valence 2.27±0.32) were used for two negative runs. There was significant valence difference between positive and negative image sets ($p \approx 0.00$). All images were displayed using the Psychopy (http://www.psychopy.org/).

Figure 1. Experimental procedure in the run.

Participants took part in 4 runs consisting of 2 positive runs and 2 negative runs. As shown in Fig. 1, every run started with a pre-scanning of 20s in favour of magnetization equilibrium. Then, participants performed 10 blocks, which included both baseline and task conditions. On the baseline condition, participants were asked to fixate at the cross on the display, and think of nothing in particular. On the task condition, images of positive or negative sets were presented centrally for 4s each, and participants tried their best to imagine experiencing the depicted situation.

B. Emotion Regulation Neurofeedback Training Using rt-fMRI

- Participants

There are 23 healthy college students (aged 22-26 years) in this experiment. All participants were right-handed and twenty-twenty vision, especially without history of neurological or psychiatric diseases. We randomly assigned subjects to an experiment group (7 males and 5 females) and a control group (8 males and 3 females). Informed consent was obtained from all participants prior to the testing, and they received financial compensation for participating in the experiment. The study was approved by the ethics committee of Henan Provincial People's Hospital.

- Experimental Paradigm

At one day prior to scanning, all subjects were required to complete a series of questionnaires, in order to assess the ability of individuals to experience emotions. Then, the selected subjects were told detailed instructions about the research purpose and the experimental paradigm, even underwent a training run outside the scanner. Moreover, these participants were asked to recollect several happy and sad impressive memory fragments and write down.

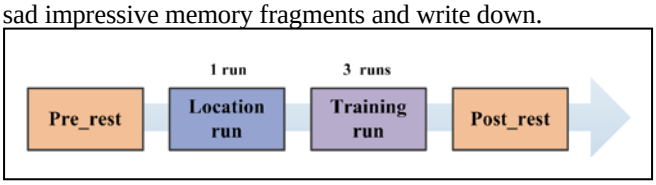

Figure 2. Experimental procedures. The experiment consists of measurement of resting state activity, location and neurofeedback training. Resting state activity measurement was followed by one location run and three training run (Pre_rest), and at the end of training runs (Post_rest).

Participants underwent four stages in the experiment (see Fig. 2). The first stage and the last stage measured participants' resting state activity, and continued six and a third minutes. In the two stages, participants were required to fixate at "+" on the display, and not to think of anything in particular. The second stage was acquired data of participants in the location run. Each participant was instructed to recall different types of emotional fragments, which were prepared at one day prior to the experiment. As for locational data, the individual feature selection mask was generated offline. After that, the most crucial part of the experiment, the third stage, was NF training. During feedback periods, participants got real-time feedback signal to understand their current emotion state, and more effectively self-regulated in the next volume.

C. Data Acquisition

During both experiments, all images were obtained using a GE Discovery MR750 (3 Tesla) scanner which was fitted with a standard 8-channel birdcage head coil at the Imaging Center of Henan Provincial People's Hospital. Foam pads were used to minimize head movements and scanner noise. BOLD signals were measured using a standard GRE-T2* EPI sequence (volume repetition time (TR) = 2000 ms, echo

time (TE) = 30 ms, flip angle (FA) = 80°). The entire brain was covered in 33 axial slices (3.5-mm thickness), matrix size was 64 × 64, and field of view was 220 mm.

D. Data Preprocessing and The Whole Brain Functional Connectivity

For all images of the first experiment and the resting-state images of the second experiment, their preprocessing was performed with SPM8 (http://www.fil.ion.ucl.ac.uk/spm). Briefly, the first step was to discard the 10 initial scans of all experiment runs, because of magnetic equilibration effects and participants adapting to the scanning noise [19]. Second, the remaining images were corrected for the acquisition time delay between slices. Then, EPI volumes were spatially realigned to correct for movement artifacts, and these volumes with a displacement of more than 3 mm or an angular rotation of greater than 3° in any direction were abandoned. Moreover, the realigned volumes were spatially normalized to the Montreal Neurological Institute (MNI) standard space by linearly registering, and smoothed using a 6 mm FWHM Gaussian spatial kernel.

Regions of interest (ROIs) were the bilateral BLA and CMA. These ROIs were created with cytoarchitectonically defined probabilistic maps of the amygdala by SPM's Anatomy Toolbox [20], as instantiated in FSL's Juelich Brain Atlas [21]. Voxels were included in the maximum probability maps with a probability more than 50%, and then assigned to the BLA and CMA in left and right hemispheres. In order to extract time series from the preprocessed fMRI data, the four ROIs were resampled to 3×3×3 mm^3 standard space. For the preprocessed data, a representative time series was obtained by averaging the fMRI time series of all voxels in the ROI. Then, functional connectivity of the whole brain was evaluated using Pearson's correlation coefficients between the representative time series and the time courses of all voxels. The Fisher's Z-transformation was performed to improve the normality.

For group statistical analyses, a two-sample t-test was employed to assess the whole-brain functional connectivity differences of four ROIs between during positive-picture condition and negative-picture condition. Furthermore, a paired t-test was conducted to compare the resting-state functional connectivity differences before and after the neurofeedback training.

E. Functional Connectivity Analysis Using Machine Learning

Feature selection is useful and important to remove garbage and improve classification performance. In this study, features come from the intersection of two-sample t-test result of the whole-brain functional connectivity in the positive and negative pictures experiment and some ROIs of limbic system on the basis of AAL atlas. ROIs of limbic system mainly contain hippocampus (HC), parahippocampal cortex (PHC), olfactory cortex, anterior cingutate (ACC), orbitofrontal cortex, medial frontal gyrus, temporal pole, thalamus (TH) and insula. These ROIs were defined with the software WFU_PickAtlas (http://www.ansir.wfubmc.edu) and also resampled to 3×3×3 mm^3 standard space. Therefore, features are functional connectivity coefficients in the intersection.

Support vector machine (SVM) which works well when the number of samples is small was adopted here for classification. Here, the binary label with 1 for positive-picture condition and -1 for negative-picture condition was used. A linear kernel SVM could reduce the risk of overfitting the data and be implemented using the LIBSVM toolbox [22] with a default value for parameter. Due to the limited number of samples, cross-validation strategy was employed to evaluate the performance of the classifier. In our study, data of 10 participants were used to train SVM model, and data of the remaining 2 participants were used as the test set. The procedure was repeated until all combinations of two participants have been left out for test. The final accuracy depended on the results of cross-validation.

III. RESULTS

A. Functional Connectivity of The Amygdala

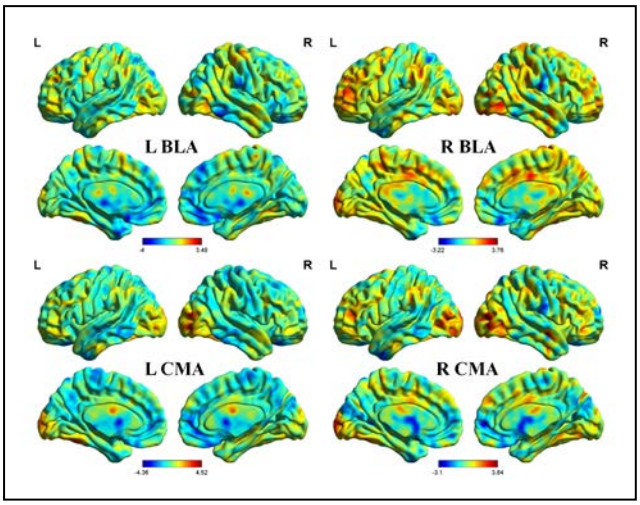

Figure 3. Distribution of whole-brain functional connectivity difference maps within groups. The color bar represents the strength of whole-brain functional connectivity difference. Brain regions with positive > negative are displayed in warm colors, while positive < negative are displayed in cool colors. Notes: L = left, R = right.

To directly examine differentiation of functional connectivity with the amygdala subregions, we computed the two-sample t-test result of positive-negative stimuli (see Fig. 3). The positive-negative stimuli had different influence on functional connectivity patterns for amygdala-limbic system. Significant differences were summarized as follows (t = 2.01, $p < 0.05$).

BLA: The left BLA seed showed significant correlation differences with a number of regions, including bilateral anterior cingulate, left inferior orbitofrontal gyrus, bilateral medial orbitofrontal gyrus, bilateral medial superior frontal gyrus, bilateral superior frontal gyrus, left insula, bilateral olfactory cortex, left parahippocampus, bilateral thalamus, left superior and middle temporal pole. The right BLA seed showed connectivity differences with right middle and

inferior temporal gyrus, left middle frontal gyrus, bilateral inferior operculum frontal gyrus, left middlt cingulate and bilateral supramarginal.

CMA: The left CMA seed showed significant correlation differences with a number of regions, including bilateral anterior cingulate, left inferior orbitofrontal gyrus, right medial orbitofrontal gyrus, bilateral medial superior frontal gyrus, bilateral superior orbitofrontal gyrus, bilateral olfactory cortex, and bilateral middle and inferior temporal gyrus. The right CMA seed showed connectivity differences with right inferior orbitofrontal gyrus, left olfactory cortex, left middle temporal pole, right middle cingulate, right middle temporal gyrus and bilateral inferior temporal gyrus.

Using four subregions of amygdala as seeds, we explored the critical connectivity for emotion recognition and regulation from task data. In MacLean's 'limbic' model of emotion, the amygdala, orbitofrontal cortex, temporal pole, insula, and other nucleus were newly increased based on the Papez circuit [23]. Functional neuroimaging studies have consistently shown that the connectivity between various regions of the prefrontal gyrus, such as medial prefrontal gyrus, and the amygdala plays an important role in processing and regulation of emotion [24].

B. Performance of Functional Connectivity for Emotion Classification

Compared the bilateral masks for extracting features, the number of left masks was much larger than the right. That's likely to associate with the lateralization of amygdala. From wide view of SVM performance, these features from masks that included left BLA-left inferior orbitofrontal gyrus, left BLA-right medial superior frontal gyrus, left BLA-bilateral superior orbitofrontal gyrus, left BLA-left olfactory cortex, left BLA-left middle temporal pole, left BLA-left superior temporal pole, left CMA-right anterior cingulate, left CMA-right medial orbitofrontal gyrus, left CMA-right medial superior frontal gyrus and left CMA-left olfactory cortex, worked better, as shown in Table I. In general, the best classification accuracy achieved by connectivity between left CMA and right medial superior frontal gyrus was 72.16%.

The results demonstrated that the critical connectivity for emotion recognition and regulation can be discriminated from whole brain functional connectivity using SVM, in agreement with our hypothesis. In recent years, machine learning methods have been used to discriminate brain disease patients from the healthy and have made progress [7-9,25-27]. Most importantly, these approaches have the advantage of taking into account the relationship among features and good potential to focus on subtle differences at group level. When to select features, masks created based on group comparison, which allows inferences at the individual level. Therefore, our analysis framework has considered both individual and group level differences in the brain. In terms of classification performance, functional connectivity of left amygdala with medial frontal gyrus, orbitofrontal gyrus and olfactory cortex mostly performed well.

TABLE I. CLASSIFICATION PERFORMANCE USING DIFFERENT MASKS

Brain masks	**Accuracy (%)**	**Brain masks**	**Accuracy (%)**
Seed: L BLA		***Seed: L CMA***	
L anterior cingulate	59.85	L anterior cingulate	62.50
L inferior orbitofrontal gyrus	66.48	R anterior cingulate	70.83
R middle orbitofrontal gyrus	63.07	R inferior orbitofrontal gyrus	60.23
L medial superior frontal gyrus	61.55	R medial orbitofrontal gyrus	67.80
R medial superior frontal gyrus	69.13	L medial superior frontal gyrus	63.07
L superior orbitofrontal gyrus	66.67	R medial superior frontal gyrus	72.16
R superior orbitofrontal gyrus	68.75	L superior orbitofrontal gyrus	62.12
L olfactory cortex	71.97	R superior orbitofrontal gyrus	62.88
R olfactory cortex	63.64	L olfactory cortex	67.05
L middle temporal pole	69.89	R olfactory cortex	65.34
L superior temporal pole	67.61	***Seed: R CMA***	
L thalamus	59.85	R inferior orbitofrontal gyrus	61.17
R thalamus	63.26	L olfactory cortex	65.91
Seed: R BLA		L middle temporal pole	61.36
L insula	64.02		

Notes: L = left, R = right.

C. Altred Functional Connectivity after Emotion Regulation Neurofeedback Training

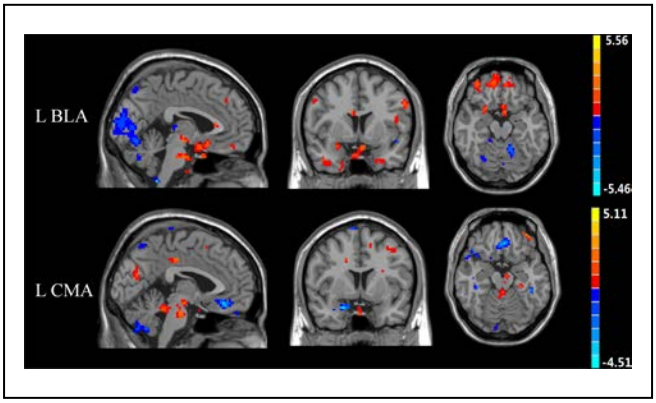

Figure 4. Distribution of altered resting-state functional connectivity maps within groups. Positive (red) indicates regions in which functional connectivity with ROIs (LBLA and LCMA) is significantly increased while negative (blue) regions in which functional connectivity is significantly decreased ($t = 2.26$, $p < 0.05$).

Results of group resting-state functional connectivity differences analysis were shown in Fig. 4. After emotion regulation training, participants showed increase in left BLA resting-state functional connectivity with bilateral anterior cingulate cortex, bilateral medial frontal gyrus, bilateral superior frontal gyrus, right dorsomedial prefrontal cortex, left parahippocampal, right middle and superior temporal gyrus and so on. In terms of left CMA resting-state functional connectivity, participants showed increase with bilateral middle frontal gyrus, right superior frontal gyrus, bilateral middle orbitofrontal gyrus, left inferior orbitofrontal gyrus, right medial superior frontal gyrus, right hippocampus, right parahippocampal and other limbic system regions.

Through the contrast between before and after emotion regulation training, we found enhanced resting-state functional connectivity between left amygdala and the prefrontal gyrus. It was reported that function of the prefrontal gyrus would be abnormal when patients with SAD, social phobia, or MDD carried out cognitive-emotional tasks [28-30]. Meanwhile, SAD patients' functional connectivity between the left amygdala and the medial orbitofrontal gyrus had obviously reduced. According to clinical studies, it indicated that OXT could enhance functional connectivity between amygdala and frontal gyrus in patients suffering from generalized SAD [31]. In addition, it was also found that the functional connectivity between amygdala and the prefrontal gyrus enhanced after patients received anti-depressant treatment [32]. In a word, resting-state functional connectivity analysis results derived from emotion regulation training data not only show the effectiveness of rt-fMRI emotion regulation, but also demonstrate reasonability of the critical connectivity we found for emotion recognition and regulation.

IV. CONCLUSIONS

Most neurological disorders are associated with changes in connectivity between brain areas. However, emotion regulation based on rt-fMRI so far has been limited by complexity of brain network. The present study extracted the core connectivity from whole emotion network using SVM, and verified its effectiveness by emotion regulation training data. The identified functional connectivity provided insight into the neural mechanisms of human emotion. Moreover, it might give a reference for the connectivity-based NF emotion regulation training, which would lead toward clinical applications in treatment of neurological and psychiatric disorders.

ACKNOWLEDGMENT

Our experimental data was collected in the Imaging Center of Henan Province. This work is supported by the National Natural Science Foundation of China (No. 61601518) and the National High Technology Research and Development Program of China (No. 2012AA011603).

REFERENCES

[1] T. English, O. P. John, S. Srivastava, J. J.Gross, "Emotion regulation and peer-rated social functioning: A 4-year longitudinal study," Journal of Research in Personality, vol. 46, Dec. 2012, pp. 780-784, doi: 10.1016/j.jrp.2012.09.006.

[2] B. J. Schmeichel and D. Tang, "The relationship between individual differences in executive functioning and emotion regulation: A comprehensive review," Motivation and Its Regulation: The Control Within, 2014, pp. 133-151, doi: 10.1177/0963721414555178.

[3] F. Liu, W. Guo, J P. Fouche, et al, "Multivariate classification of social anxiety disorder using whole brain functional connectivity," Brain Structure and Function, vol. 220, Jan. 2015, pp. 101-115, doi: 10.1007/s00429-013-0641-4.

[4] APA, "Diagnostic and statistical manual of mental disorders: DSM-IV," American Psychiatric Publishing, Inc.,1994.

[5] B. Biswal, F. Zerrin Yetkin, V. M. Haughton and J. S. Hyde, "Functional connectivity in the motor cortex of resting human brain using echo-planar mri ," Magnetic resonance in medicine, vol. 34, Oct. 1995, pp. 537-541, doi: 10.1002/mrm.1910340409.

[6] M. D. Fox and M.Greicius, "Clinical applications of resting state functional connectivity," Frontiers in systems neuroscience, vol. 4, Jun. 2010, p. 19, doi: 10.3389/fnsys.2010.00019.

[7] Y. Liu, M. Liang, Y. Zhou, et al, "Disrupted small-world networks in schizophrenia," Brain, vol. 131, Feb. 2008, pp. 945-961, doi: 10.1093/brain/awn018.

[8] W. Guo, F. Liu, Z. Xue, et al, "Abnormal resting-state cerebellar-cerebral functional connectivity in treatment-resistant depression and treatment sensitive depression," Progress in Neuro-Psychopharmacology and Biological Psychiatry, vol. 44, Jan. 2013, pp.51-57, doi: 10.1016/j.pnpbp.2013.01.010.

[9] B. Jie, D. Zhang, C. Y. Wee, D. G. Shen, "Topological graph kernel on multiple thresholded functional connectivity networks for mild cognitive impairment classification," Human brain mapping, vol. 35, Sep. 2014, pp. 2876-2897, doi: 10.1002/hbm.22353.

[10] S. Haller, K.O. Lovblad, P. Giannakopoulos, D. V. D. Ville, "Multivariate pattern recognition for diagnosis and prognosis in clinical neuroimaging: state of the art, current challenges and future trends," BrainTopogr, vol. 27, Mar. 2014, pp. 329-337, doi: 10.1007/s10548-014-0360-z.

[11] V. Zotev, R. Phillips, K. D. Young, et al, "Prefrontal control of the amygdala during real-time fMRI neurofeedback training of emotion regulation," PloS One, vol. 8, Nov. 2013, p. e79184, doi:

10.1371/journal.pone.0079184.

[12] K. C. Kadosh, Q. Luo, C. de Burca, et al, "Using real-time fMRI to influence effective connectivity in the developing emotion regulation network," NeuroImage, vol. 125, Oct. 2016, pp. 616-626, doi: 10.1016/j.neuroimage.2015.09.070 .

[13] J. W. Papez, "A proposed mechanism of emotion," Archives of Neurology & Psychiatry, vol: 38, Nov. 1937, pp. 725-734, doi: 10.1001/archneurpsyc.1937.02260220069003.

[14] S. J. Banks, K. T Eddy, M. Angstadt, P. J. Nathan, K. L. Phan, "Amygdala–frontal connectivity during emotion regulation," Social cognitive and affective neuroscience, vol. 2, Jan. 2007, pp. 303-312, doi: 10.1093/scan/nsm029 .

[15] Y. Shao, Y. Lei, L. Wang, et al, "Altered resting-state amygdala functional connectivity after 36 hours of total sleep deprivation," PloS one, vol. 9, Nov. 2014, p. e112222, doi: 10.1371/journal.pone.0112222.

[16] A. K. Roy, Z. Shehzad, D. S. Margulies, et al, "Functional connectivity of the human amygdala using resting state fMRI," Neuroimage, vol.45, Apr. 2009, pp. 614-626, doi: 10.1016/j.neuroimage.2008.11.030.

[17] S. Qin, C. B. Young, K. Supekar, L. Q. Uddin, V. Menon, "Immature integration and segregation of emotion-related brain circuitry in young children," Proceedings of the National Academy of Sciences, vol. 109, Apr. 2012, pp. 7941-7946, doi: 10.1073/pnas.1120408109.

[18] S. Ruiz, S. Lee, S R. Soekadar, et al, "Acquired self-control of insula cortex modulates emotion recognition and brain network connectivity in schizophrenia," Human Brain Mapping, vol. 34, Jan. 2013, pp. 200-212, doi: 10.1002/hbm.21427.

[19] F. Liu, W. Guo, L. Liu, et al, "Abnormal amplitude low-frequency oscillations in medication-naive, first-episode patients with major depressive disorder: a resting-state fMRI study," Journal of affective disorders, vol. 146, Oct. 2013, pp. 401-406, doi: 10.1016/j.jad.2012.10.001.

[20] S. B. Eickhoff, K. E. Stephan, H. Mohlberg, et al, "A new SPM toolbox for combining probabilistic cytoarchitectonic maps and functional imaging data," Neuroimage, vol. 25, Mar. 2005, pp. 1325-1335, doi: 10.1016/j.neuroimage.2004.12.034.

[21] K. Amunts, O. Kedo, M. Kindler, et al, "Cytoarchitectonic mapping of the human amygdala, hippocampal region and entorhinal cortex: intersubject variability and probability maps," Anatomy and embryology, vol. 210, Oct. 2005, pp. 343-352, doi: 10.1007/s00429-005-0025-5.

[22] C. C. Chang and C. J. Lin, "LIBSVM: a library for support vector machines," ACM Transactions on Intelligent Systems and Technology (TIST), vol. 2, Apr. 2011, p. 27, doi: 10.1145/1961189.1961199.

[23] P. D. MacLean, "Psychosomatic disease and the 'visceral brain': recent developments bearing on the papez theory of emotion," Psychosomatic Medicine, vol. 11, Nov. 1949, pp. 338-353, doi: 10.1097/00006842-194911000-00003.

[24] M. L. Phillips, C. D. Ladouceur, W. C. Drevets, "A neural model of voluntary and automatic emotion regulation: implications for understanding the pathophysiology and neurodevelopment of bipolar disorder," Molecular psychiatry, vol. 13, Sep. 2008, pp. 833-857, doi: 10.1038/mp.2008.65.

[25] L. L. Zeng, H. Shen, L. Liu, D. W. Hu, "Unsupervised classification of major depression using functional connectivity MRI," Human brain mapping, vol. 35, Apr. 2014, pp. 1630-1641, doi: 10.1002/hbm.22278.

[26] F. Liu, B. Xie, Y. Wang, et al, "Characterization of post-traumatic stress disorder using resting-state fMRI with a multi-level parametric classification approach," Brain topography, vol. 28, Jul. 2015, pp. 221-237, doi: 10.1007/s10548-014-0386-2.

[27] C. Y. Wee, P. T. Yap, D. Zhang., L Wang, D. G. Shen, "Group-constrained sparse fMRI connectivity modeling for mild cognitive impairment identification," Brain Structure and Function, vol. 219, Mar. 2014, pp. 641-656, doi: 10.1007/s00429-013-0524-8.

[28] A. Hahn, P. Stein, C. Windischberger, et al, "Reduced resting-state functional connectivity between amygdala and orbitofrontal cortex in social anxiety disorder," Neuroimage, vol. 56, Feb. 2011, pp. 881-889, doi: 10.1016/j.neuroimage.2011.02.064.

[29] L. R. Demenescu, R. Kortekaas, H. R. Cremers, et al. "Amygdala activation and its functional connectivity during perception of emotional faces in social phobia and panic disorder," Journal of psychiatric research, vol. 47, Mar. 2013, pp. 1024-1031, doi 10.1016/j.jpsychires.2013.03.020.

[30] M. D. Greicius, B. H. Flores, V. Menon, et al, "Resting-state functional connectivity in major depression: abnormally increased contributions from subgenual cingulate cortex and thalamus," Biological psychiatry, vol. 62, Oct. 2007, pp. 429-437, doi: 10.1016/j.biopsych.2006.09.020.

[31] S. Dodhia, A. Hosanagar, D. A. Fitzgerald, et al, "Modulation of resting-state amygdala-frontal functional connectivity by oxytocin in generalized social anxiety disorder," Neuropsychopharmacology, vol. 39, Mar. 2014, pp. 2061-2069, doi: 10.1038/npp.2014.53.

[32] G. S. Dichter, D. Gibbs and M. J. Smoski, "A systematic review of relations between resting-state functional-MRI and treatment response in major depressive disorder," Journal of affective disorders, vol. 172, Feb. 2015, pp. 8-17, doi: 10.1016/j.jad.2014.09.028.